

Electronic Supplementary Information

Enhanced reversibility of H₂ sorption in nanoconfined complex metal hydrides by alkali metal addition

Jinbao Gao^a, Peter Ngene^a, Inge Lindemann^b, Oliver Gutfleisch^b, Krijn P. de Jong^a, Petra E. de Jongh^{*a}

^a*Inorganic Chemistry and Catalysis, Debye Institute for Nanomaterials Science, Utrecht University, Universiteitweg 99, 3584 CJ, Utrecht, The Netherlands. E-mail: p.e.dejongh@uu.nl*

^b*Functional Magnetic Materials and Hydrides Group, IFW Dresden, Institute for Metallic Materials, Helmholtzstraße 20, D-01069 Dresden, Germany.*

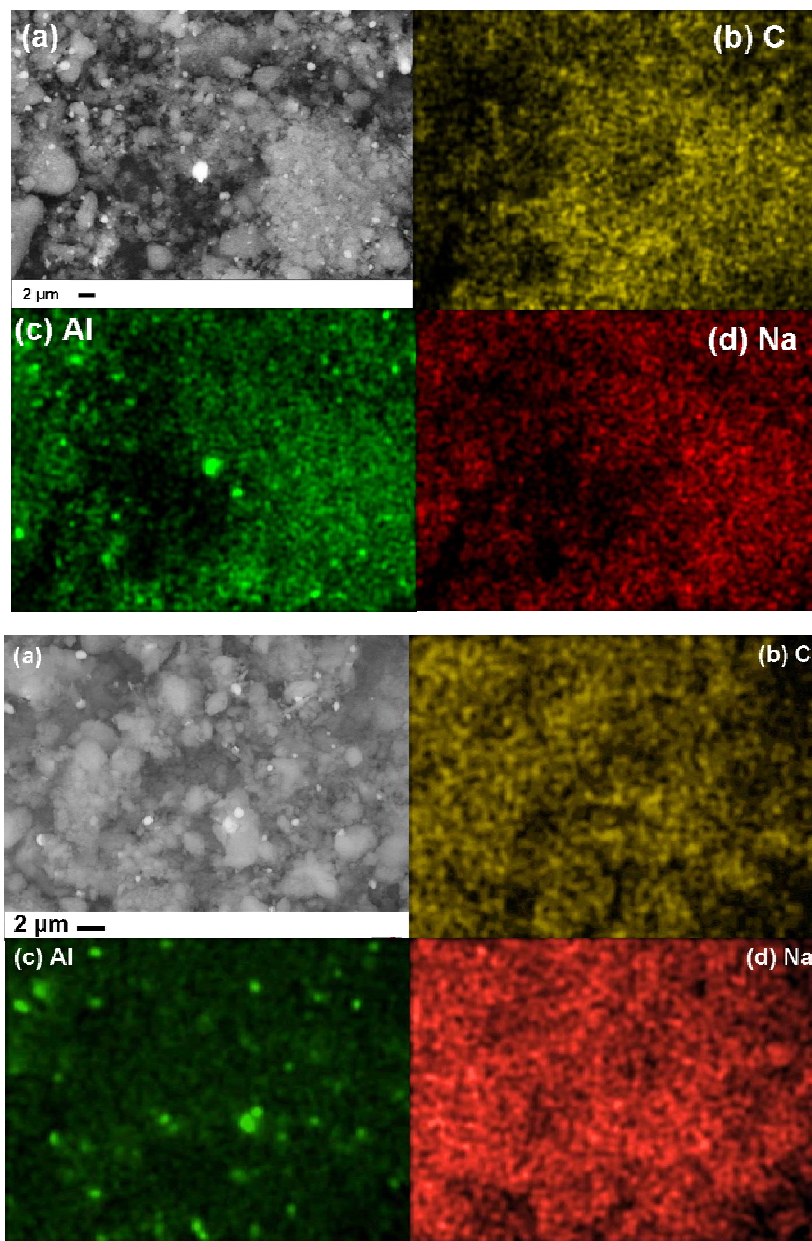


Fig. S1 Scanning electron micrographs of melt infiltrated 20 wt % NaAlH_4/C nanocomposites (upper images) and rehydrogenated sample with backscattered electrons imaging (a) and energy-dispersive X-ray mappings of C (b), Al (c) and Na (d). For the melt infiltrated sample, Al and Na have similar distributions over the carbon support after melt infiltration. The presence of Al crystallites (bright spots in mapping (c)) is attributed to the reactions between NaAlH_4 and impurities in carbon during melt infiltration. For the rehydrogenated sample, Na disperses very well over carbon. Less large Al containing particles are observed compared to that of dehydrogenated sample, suggesting part of Al is reconverted to NaAlH_4 upon rehydrogenation.

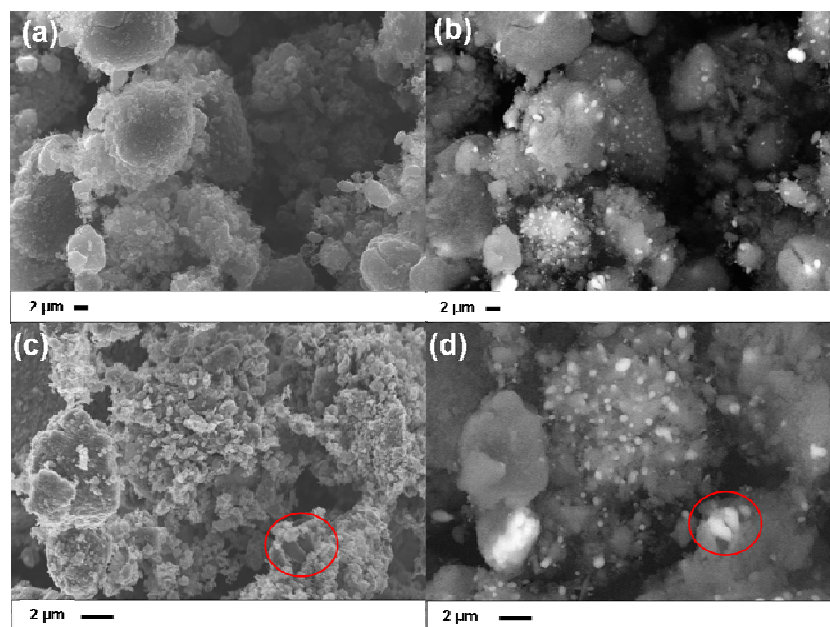


Fig. S2 Scanning electron micrographs of dehydrogenated 20 wt % NaAlH₄/C nanocomposites (a), (c) and corresponding images of same area with backscattered electron imaging (b), (d), showing that some Al particles are located on the outer surface of the carbon particles (examples indicated by circles in image(c) and (d)).

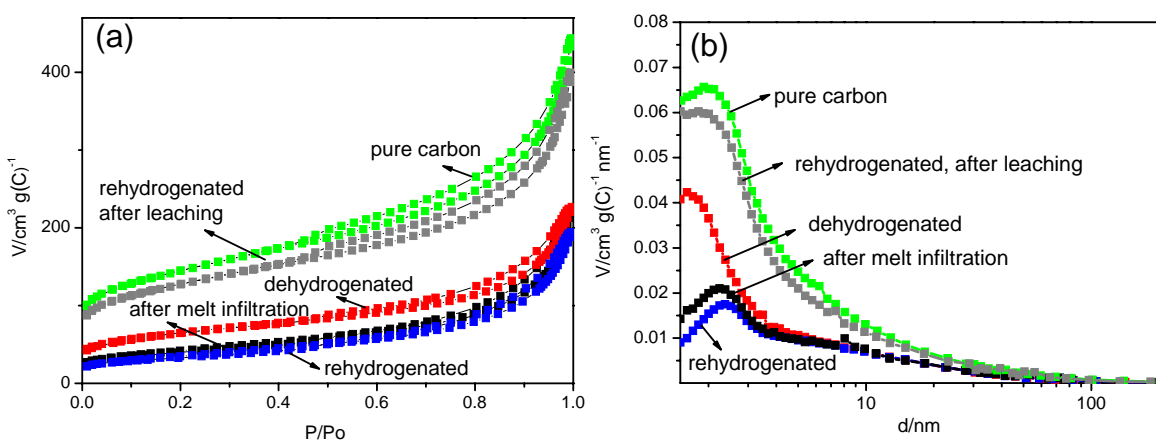


Fig. S3 N₂ physisorption results for sample 20 wt % NaAlH₄/C, comparing the porosity after melt infiltration, dehydrogenation, rehydrogenation and after leaching the rehydrogenated sample: (a) isotherm; (b) pore size distribution. Carbon material gained porosity in the small pore range after dehydrogenation and lost porosity again after rehydrogenation. The porosity of carbon was almost fully recovered after leaching, indicating that the carbon structure was preserved during the H₂ sorption cycle.

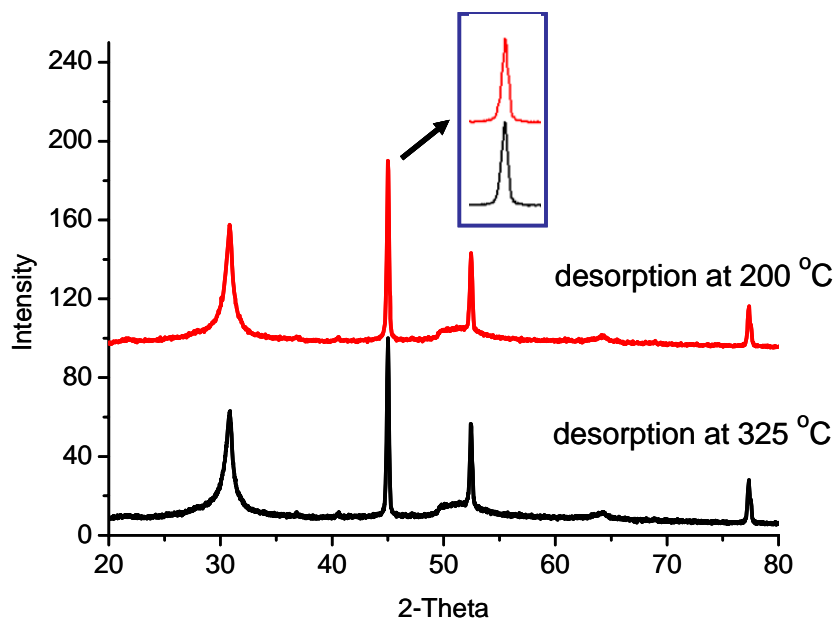


Fig. S4 XRD patterns of melt infiltrated nanocomposites (20 wt % NaAlH₄/C) after dehydrogenation at different temperature in Ar atmosphere. The presence of sharp Al diffraction lines indicates that large Al crystallites are formed at these dehydrogenation temperatures.

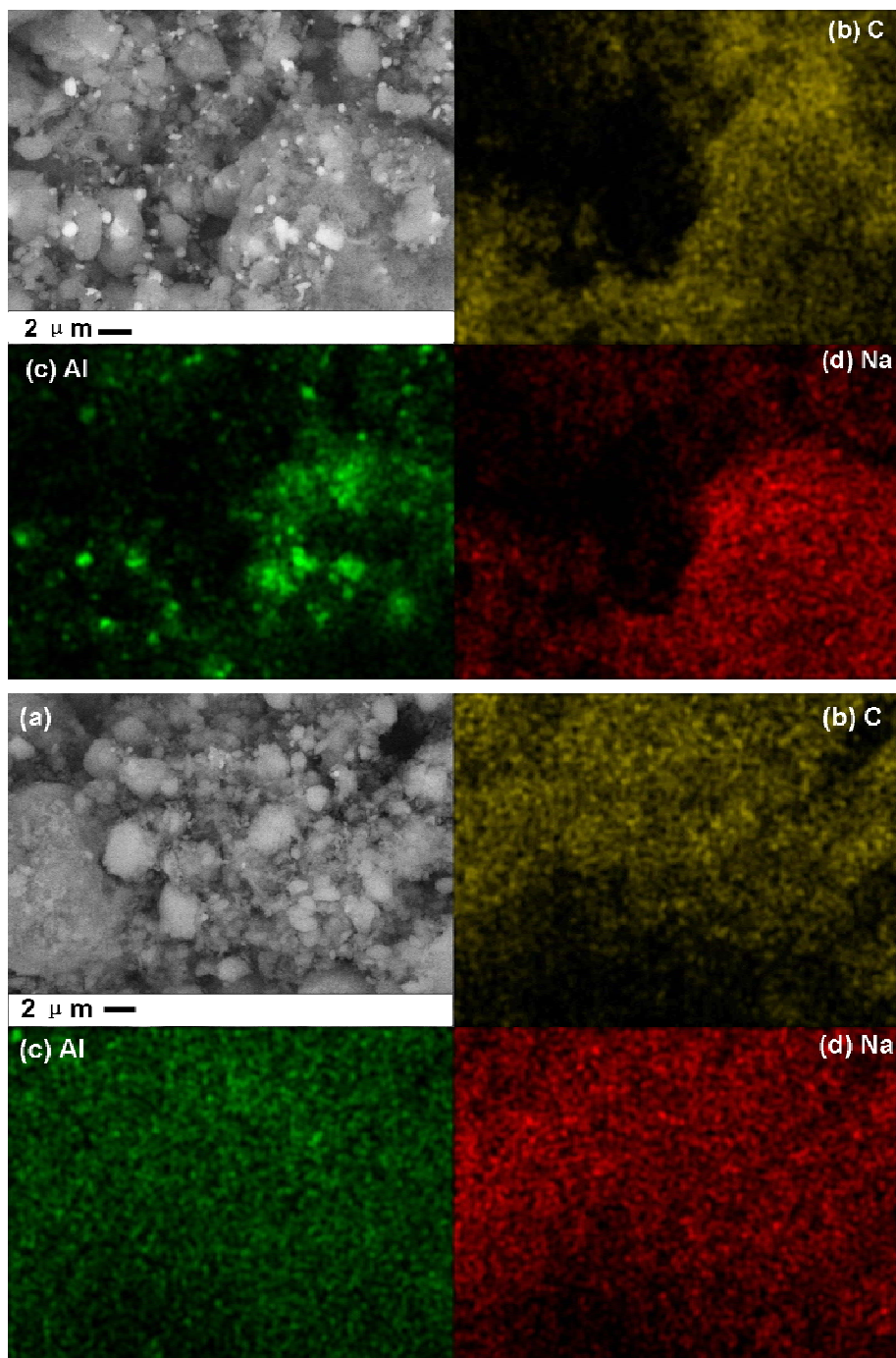


Fig. S5 Scanning electron micrographs of dehydrogenated (upper images) and rehydrogenated nanocomposites (with Na/Al molar ratio of 1.3) with backscattered electrons imaging (a) and energy-dispersive X-ray mappings of C (b), Al (c) and Na (d). The results show Na well dispersed over the carbon support in both samples. Some large Al containing particles are observed in the dehydrogenated sample, while no large Al containing particles are found in the rehydrogenated sample.

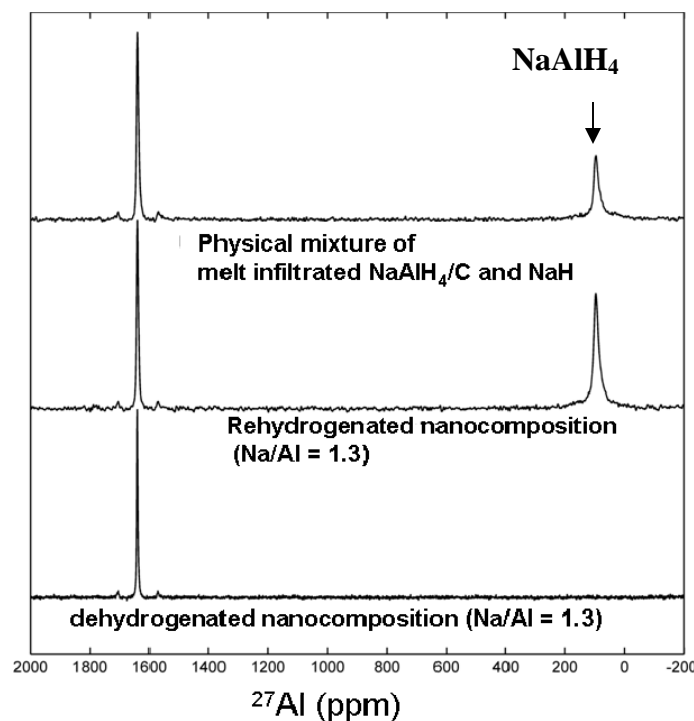


Fig. S6 ^{27}Al NMR of rehydrogenated nanocomposites (Na/Al = 1.3). Results of starting sample (physical mixture of NaAlH_4/C and NaH) and subsequently dehydrogenated sample are also shown as references. The results indicate that no significant microstructural change for the reformed NaAlH_4 compared to that of starting sample.

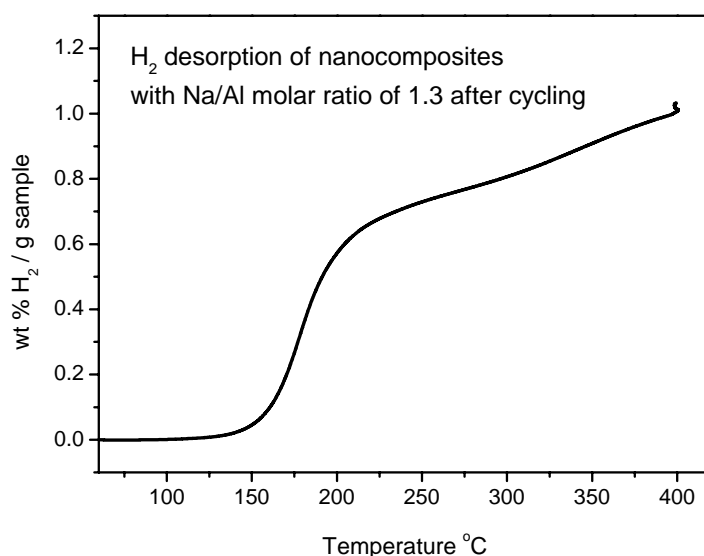


Fig. S7 H_2 desorption of nanocomposites with Na/Al molar ratio of 1.3 after cycling (detailed experimental conditions see Fig. S5) by increasing the temperature to 400 $^\circ\text{C}$ under 1 bar Ar. 1.04 wt% H_2 / g sample (5.2 wt% H_2 /g NaAlH_4) was released suggesting almost full H_2 cycling capacity was achieved after cycling.

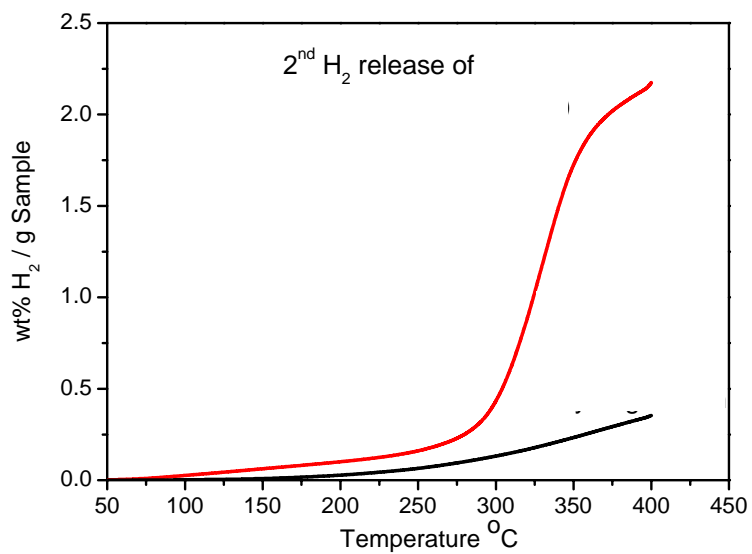


Fig. S8 Second H₂ release of 20 wt% LiBH₄/(C+Li/LiH) and H₂ release of Li/LiH containing carbon ((Li/LiH)/C) after rehydrogenation under 50 bar H₂ pressure and 325 °C for 5 h.